

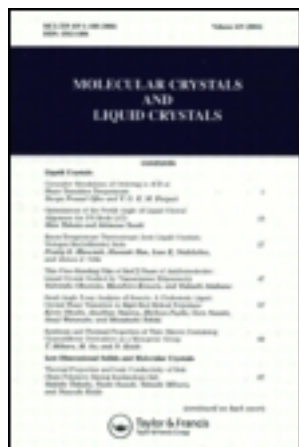
This article was downloaded by: [University of Haifa Library]

On: 17 August 2012, At: 10:22

Publisher: Taylor & Francis

Informa Ltd Registered in England and Wales Registered Number: 1072954

Registered office: Mortimer House, 37-41 Mortimer Street, London W1T 3JH, UK



## Molecular Crystals and Liquid Crystals Science and Technology. Section A. Molecular Crystals and Liquid Crystals

Publication details, including instructions for authors and subscription information:

<http://www.tandfonline.com/loi/gmcl19>

### Assembly of Metal Complexes

Hiroki Oshio <sup>a</sup>, Takashi Hikichi <sup>a</sup>, Taira Yaginuima <sup>a</sup>, Hironori Onodera <sup>a</sup>, Masashi Yamamoto <sup>a</sup> & Tasuku Ito <sup>a</sup>

<sup>a</sup> Department of Chemistry, Graduate School of Science, Tohoku University, Aoba-ku, Sendai, 980-8578, Japan

Version of record first published: 24 Sep 2006

To cite this article: Hiroki Oshio, Takashi Hikichi, Taira Yaginuima, Hironori Onodera, Masashi Yamamoto & Tasuku Ito (1999): Assembly of Metal Complexes, Molecular Crystals and Liquid Crystals Science and Technology. Section A. Molecular Crystals and Liquid Crystals, 334:1, 497-509

To link to this article: <http://dx.doi.org/10.1080/10587259908023346>

PLEASE SCROLL DOWN FOR ARTICLE

Full terms and conditions of use: <http://www.tandfonline.com/page/terms-and-conditions>

This article may be used for research, teaching, and private study purposes. Any substantial or systematic reproduction, redistribution, reselling, loan, sub-licensing, systematic supply, or distribution in any form to anyone is expressly forbidden.

The publisher does not give any warranty express or implied or make any representation that the contents will be complete or accurate or up to date. The accuracy of any instructions, formulae, and drug doses should be independently verified with primary sources. The publisher shall not be liable for any loss, actions, claims, proceedings, demand, or costs or damages whatsoever or howsoever caused arising directly or indirectly in connection with or arising out of the use of this material.

## Assembly of Metal Complexes

HIROKI OSHIO, TAKASHI HIKICHI, TAIRA YAGINUIMA,  
HIRONORI ONODERA, MASASHI YMAMAMOTO and  
TASUKU ITO

*Department of Chemistry, Graduate School of Science, Tohoku University,  
Aoba-ku, Sendai 980-8578, Japan*

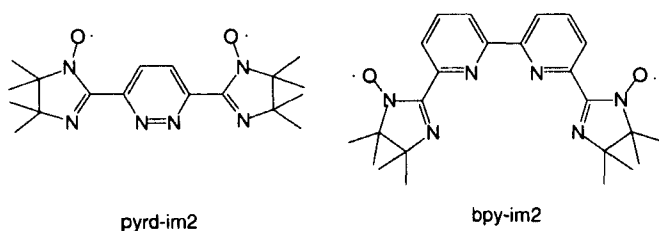
The reactions of silver(I) hexafluorophosphate with imino nitroxyl diradicals yield complexes of  $[\text{Ag}_2(\text{pyrd-im}2)_2](\text{PF}_6)_2 \cdot 2\text{CH}_3\text{OH}$  (**1**) and  $[\text{Ag}_2(\text{bpy-im}2)_2](\text{PF}_6)_2 \cdot \text{CH}_3\text{OH}$  (**2**) ( $\text{pyrd-im}2 = 3,6\text{-bis(1'-oxyl-4',4'',5',5''-tetramethyl-4',5'-dihydro-1'H-imidazol-2'-yl)pyridazine}$ ) and  $\text{bpy-im}2 = 2,2'\text{-bis(1'-oxyl-4',4'',5',5''-tetramethyl-4',5'-dihydro-1'H-imidazol-2'-yl)bipyridine}$ ). Complexes **1** and **2** have four radicals being double-helically assembled by the coordination to the silver ions. Magnetic susceptibility measurements revealed a strong antiferromagnetic interaction ( $-70.8(7)$  cm with  $H = 2JS_1 \cdot S_2$ ) in **1** being operative through the pyridazine group, which was understood by the spin polarization mechanism. The reaction of  $\text{MnSO}_4 \cdot 4\text{H}_2\text{O}$  with  $\text{K}_2\text{CrO}_4$  in water yielded highly crystalline black **3**. X-ray crystallographic study revealed that **3** has the chemical formula  $\text{K}[\text{Mn}_2(\mu\text{-CrO}_4)_2(\mu\text{-OH})_2]$ , which implies that the manganese ions are mixed valent Mn(II,III). Magnetic susceptibility measurement reveals that the antiferromagnetic interactions are operative without antiferromagnetic ordering and the exchange coupling constant was estimated to be  $-1.4 \text{ cm}^{-1}$ .

**Keywords:** metal radical complex; chromate bridge

### INTRODUCTION

Supramolecular chemistry of coordination compounds is the subject of intense research interest.<sup>1</sup> It has been known for several years that self-assembly of oligopyridyl strand with  $\text{Ag}^1$  and  $\text{Cu}^1$  ions gave well organized molecular architecture like inorganic grid,<sup>2</sup> double-,<sup>3</sup> and triple-<sup>4</sup> stranded metal helicates. General feature of such diamagnetic metal ions as a component of the self-

assembled system is that the tetrahedral coordination algorithm can give helicate formation of the oligopyridyl strands. If the organic radicals are introduced into such oligopyridyl strands, the radicals are self-assembled to form radical-supramolecules. In the first part of this paper, silver(I) complexes with double-stranded radical helicates of diradicals were reported. Diradical ligands used were diimino nitroxied linked by pyridazine and bipyridine, respectively, and depicted below.



On the other hand, mixed-valent manganese clusters have been extensively studied from both bioinorganic and solid state chemical view points. Competing magnetic interactions in some  $\mu_3$ -oxide bridged manganese clusters show frustration in the spin alignment.<sup>5</sup> Large magnetic anisotropy in these giant spin clusters or “superparamagnets” results in quantum magnetic hysteresis<sup>6</sup> and spin tunneling<sup>7</sup> between spin states. A chromate ion,  $[\text{CrO}_4]^{2-}$ , has been known to act as a bridging ligand. When the  $[\text{CrO}_4]^{2-}$  ion bridges  $\text{Cu(II)}$  or  $\text{Ni(II)}$  ions in  $[\{\text{Cu}(\text{acpa})\}_2(\mu\text{-CrO}_4)]$  (acpa = tridentate Schiff base)<sup>8</sup> and *catena*-( $\mu\text{-CrO}_4\text{-O,O'}$ )[ $\text{Ni}(\text{cyclam})$ ],<sup>9</sup> respectively, ferromagnetic interactions ( $J = +14.6$   $+0.6$   $\text{cm}^{-1}$ , respectively) were operative through the chromate ions. Propagation of the ferromagnetic interactions in  $d_9$ -spin system like  $\text{Cu(II)}$  and  $\text{Ni(II)}$  complexes can be interpreted by the accidental orbital degeneracy of the metal ions, which results from the strictly degenerate HOMO of the  $[\text{CrO}_4]^{2-}$ . In mixed  $d\pi$  and  $d\sigma$  systems, however, chromate ions act as an antiferromagnetic coupler, for example, in a di-ferric compound,  $[\text{LFe}^{\text{III}}-(\mu\text{-CrO}_4)_3\text{-Fe}^{\text{III}}\text{L}]$  ( $\text{L} = 1,4,7\text{-trimethyl-1,4,7-triazacyclononane}$ ), the weakly antiferromagnetic interaction ( $2J = -15.0$   $\text{cm}^{-1}$  and  $H = -2JS_1S_2$ ) was

observed.<sup>10</sup> In the second part this paper, we report synthesis, structure and magnetic property of a mixed valent Mn(II,III) complex with a 2D structure.

## EXPERIMENTAL

### Syntheses

[Ag<sub>2</sub>(pyrd-im2)<sub>2</sub>](PF<sub>6</sub>)<sub>2</sub>·2CH<sub>3</sub>OH **1** and [Ag<sub>2</sub>(bpy-im2)<sub>2</sub>](PF<sub>6</sub>)<sub>2</sub>·CH<sub>3</sub>OH **2**. Ligands pyrd-im2 (180 mg, 0.5 mmol) and bpy-im2 (217 mg, 0.5 mmol) were, respectively, added to the methanol solution (50 ml) of AgPF<sub>6</sub> (126 mg, 0.5 mmol). After stand for overnight the resulting dark red microcrystallines were filtered off. Recrystallization in methanol gave dark red tablets, one of which was subjected to the X-ray structural analysis.

K[Mn<sub>2</sub>(μ-CrO<sub>4</sub>)<sub>2</sub>(μ-OH)<sub>2</sub>] **3**. Reaction of MnSO<sub>4</sub>·4H<sub>2</sub>O with K<sub>2</sub>CrO<sub>4</sub> in water yielded highly crystalline black **3**.

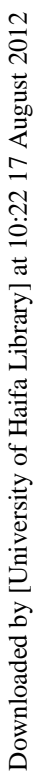
## RESULTS AND DISCUSSION

### Description of the Structure.

[Ag<sub>2</sub>(pyrd-im2)<sub>2</sub>](PF<sub>6</sub>)<sub>2</sub>·2CH<sub>3</sub>OH **1** and [Ag<sub>2</sub>(bpy-im2)<sub>2</sub>](PF<sub>6</sub>)<sub>2</sub>·CH<sub>3</sub>OH **2**.

Complexes **1** and **2** crystallize in the monoclinic space group *Cc*, and orthorhombic space group *Pbca*, respectively. The absolute structure for **1** was determined by using the Flack's parameter,<sup>11</sup> which was estimated to be 0.08(3) for the presented structure. The crystal structure determinations for **1** and **2** show the compounds to be composed of a dimeric cation of [Ag<sub>2</sub>(pyrd-im2)<sub>2</sub>]<sup>2+</sup> (Figure 1) and [Ag<sub>2</sub>(bpy-im2)<sub>2</sub>]<sup>2+</sup> (Figure 2), respectively, which are best described as double-stranded helicates with the coordinated ligands being twisted around the Ag(1)-Ag(2) axis. In **1** and **2**, two silver ions doubly bridged by the diradicals are separated by 5.352(2) and 6.025(2) Å, respectively, and the dimeric molecules have four imino nitroxides. In **1**, the silver ions have two coordinated nitrogen atoms of the imino nitroxide groups. Bond lengths and angles of silver ions and coordinated nitrogen atoms are in the range of 2.129(4) - 2.163(5) Å and of 152.5(2) - 156.7(2)°, respectively,

Downloaded by [University of Haifa Library] at 10:22 17 August 2012



Downloaded by [University of Haifa Library] at 10:22 17 August 2012

Downloaded by [University of Haifa Library] at 10:22 17 August 2012

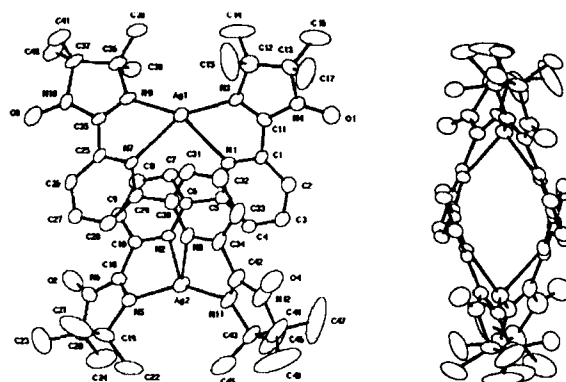


FIGURE 2. ORTEP diagram of  $[\text{Ag}_2(\text{bpy-im2})_2](\text{PF}_6)_2 \cdot \text{CH}_3\text{OH}$  **2**.

### $\text{K}[\text{Mn}_2(\mu\text{-CrO}_4)_2(\mu\text{-OH})_2]$ **3**.

X-ray crystallographic revealed that **3** has a chemical formula of  $\text{K}[\text{Mn}_2(\mu\text{-CrO}_4)_2(\mu\text{-OH})_2]$ , which implies the manganese ions being Mn(II,III) mixed valent. Complex **1** crystallizes in the monoclinic space group  $C2/m$ .

Manganese and potassium ions locate on the crystallographic inversion and twofold rotation axis, respectively, while the  $[\text{CrO}_4]^{2-}$  and hydroxide groups locate on the mirror plane. In **3**, manganese ions are bridged by hydroxide and chromate ions to form a 2D structure (Figure 3). Two oxygen atoms of O4 and O3 from  $\text{OH}^-$  and  $[\text{CrO}_4]^{2-}$  ions and O2-Cr-O2' bond bridge manganese ions to form a chain like structure along the b-axis. The manganese ions in the chains are doubly linked by O2-Cr-O3 bonds and, as the result, **3** forms a layer structure on the ab-plane, where the layers are separated by 7.751(1) Å.

Octahedral coordination sites of the manganese ion were occupied by oxygen atoms with bond lengths of 2.139(3) - 2.229(4) Å. Bridging angle of hydroxide (Mn-O3-Mn) and oxide (Mn-O4-Mn) of  $[\text{CrO}_4]^{2-}$  ions are 99.9(2)° and 94.5(2)°, respectively. Coordination geometry of the chromate ion is tetrahedron of which three oxygen atoms bridge manganese ions while the remainder of oxygen atoms with the shortest bond length of 1.605(4) Å remains non-coordinated. It is uncertain from X-ray analysis whether the

valence electrons are trapped on certain atoms or delocalized on the whole solids, although the X-ray analysis shows the only one kind of crystallographically independent manganese ion.

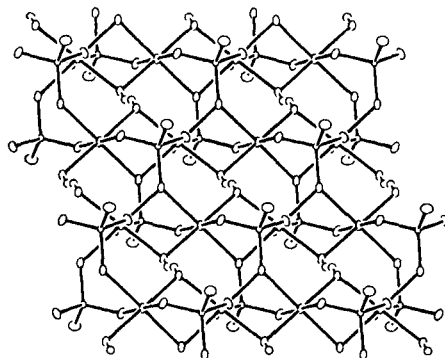


FIGURE 3. ORTEP diagram of  $\text{K}[\text{Mn}_2(\mu\text{-CrO}_4)_2(\mu\text{-OH})_2]$  **3**.

### **Magnetic Properties**

$[\text{Ag}_2(\text{pyrd-im}2)_2](\text{PF}_6)_2 \cdot 2\text{CH}_3\text{OH}$  **1** and  $[\text{Ag}_2(\text{bpy-im}2)_2](\text{PF}_6)_2 \cdot \text{CH}_3\text{OH}$  **2**.

Temperature dependence of magnetic susceptibility of the compounds were measured down to 2.0 K. Room temperature  $\chi_m T$  value of **2** is  $1.49 \text{ emu}^{-1} \text{ K mol}^{-1}$ , which would be expected for the isolated four spin system, and  $\chi_m T$  remains at constant plateau down to 50 K, then decreases to a value of  $0.7 \text{ emu}^{-1} \text{ K mol}^{-1}$  at 2.0 K. Magnetic data of **2** was analyzed by the four spin model with two exchange coupling constants  $J_1$  and  $J_2$  representing magnetic interactions through the silver ions and bipyridine groups ( $H = -2J_1(S_1 \cdot S_2 + S_3 \cdot S_4) - 2J_2(S_1 \cdot S_3 + S_2 \cdot S_4)$ ). The best fitting parameters of both  $J_1$  and  $J_2$  values are  $-1.4(1) \text{ cm}^{-1}$ . The magnetic susceptibility data of **1** are shown in the form of  $\chi_m T$  vs.  $T$  and  $\chi_m$  vs.  $T$  plots (Figure 4). The  $\chi_m T$  value of **1** steadily decreases as the temperature lowered, reaching a value of  $0.005 \text{ emu K mol}^{-1}$  at 2.0 K, which is indicative of intramolecular antiferromagnetic interactions. The closest intermolecular contact of nitroxyl groups is  $4.3 \text{ \AA}$ , which exclude the



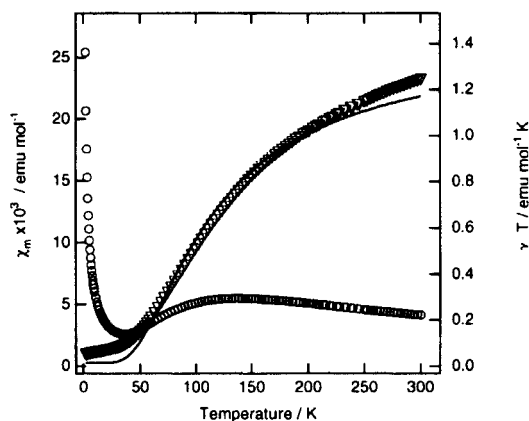


FIGURE 4. Plots of  $\chi_m T$  and  $\chi_m$  vs  $T$  for  $[\text{Ag}_2(\text{pyrd-im}2)_2](\text{PF}_6)_2 \cdot 2\text{CH}_3\text{OH}$  **1**. Solid lines correspond to the best fit curves by using the parameters given in the text.

presence of substantial intermolecular magnetic interactions. The two exchange parameters  $J_1$  and  $J_2$  through the silver ions and pyridazine groups, respectively, were used to analyze the magnetic data. The magnetic interaction of the imino nitroxides through the silver ions is considered to be the same order as that of **2**, because the coordination bond length and angles of the imino nitroxides in **1** are very similar to those of **2**. The exchange coupling constant through the silver ions was, therefore, fixed to  $-1.4 \text{ cm}^{-1}$  in the analysis of the magnetic data of **1**.<sup>12</sup> The least square calculation, where the contribution of paramagnetic impurity ( $p$ ) was included and the  $g$ -value was fixed to 2.0, yielded the best fit parameters of  $J_2 = -70.8(7) \text{ cm}^{-1}$  and  $p = 0.03(1)$ . The significant antiferromagnetic interactions are propagated by the pyridazine ring, which can be understood by the spin-polarization mechanism.<sup>13</sup>

The amplitude of the antiferromagnetic interaction in **1** is twice as large as that for the reported diradicals, NITPh(4-NIT) ( $J = 72.3 \text{ cm}^{-1}$ ,  $H = JS_1 \cdot S_2$ ), in which two nitronyl nitroxides are linked by the phenyl group in its para-

positions (NITPh(4-NIT) = 1,4-bis-(1'-oxyl-3'-oxido-4',4',5',5'-tetramethyl-4,5-dihydro-1*H*-imidazol-2'-yl)benzene).<sup>14</sup> Dihedral angles of radical moieties with bridging aromatic rings affect the strength of magnetic interactions through the bridges. It should be noted that the dihedral angle of imino nitroxyl and pyridazyl groups in pyrd-im2 (28.7(2) and 31.1(2)°) are comparable to those of the nitronyl nitroxyl and phenyl planes in NITPh(4-NIT) (36.7(1) and 28.2(1)°). In order to understand different magnetic behaviors of the diradicals, PM3 MO (= molecular orbital) calculations with the RHF level were done for diradicals of imino (-im2) and nitronyl (-nit2) nitroxides which are linked with para-positions of pyridazyl (pyrd-) and phenyl (ph-)groups, and compounds calculated were abbreviated as pyrd-im2, pyrd-nit2, ph-im2 and ph-nit2 (Figure 5).<sup>15</sup> Homo-lumo energy gaps, which are representative of the strength of antiferromagnetic interactions,<sup>16</sup> are calculated to be 2.099, 2.082, 1.917, and 1.880 eV for pyrd-im2, pyrd-nit2, ph-im2 and ph-nit2, respectively (Figure 4). The observed stronger antiferromagnetic interaction in pyrd-im2 compared with NITPh(4-NIT) (= ph-nit2) can be explained by the larger homo-lumo energy gaps for pyrd-im2. Net charge analyses of the diradicals reveal that the pyridazyl group are less positive than the phenyl groups (Figure 5), and this is due to the larger electronegativity of the pyridazyl nitrogen atoms. The more spin delocalization occurs in pyridazyl bridged diradical (pyrd-im2), and the stronger antiferromagnetic interaction is propagated through the pyridazyl group than that through the phenyl group in NITPh(4-NIT). On the other hand, considering the less positive charges and the larger homo-lumo energy gaps for imino nitroxides compared with nitronyl nitroxides, it is suggested that the resonance structure of nitronyl nitroxide and electron withdrawing effect of the nitronyl oxygen atom prevent the spin delocalization onto the linking groups, hence, among the diradicals linked by aromatic groups the imino nitroxides are expected to show the stronger antiferromagnetic interaction than that of the nitronyl nitroxides.

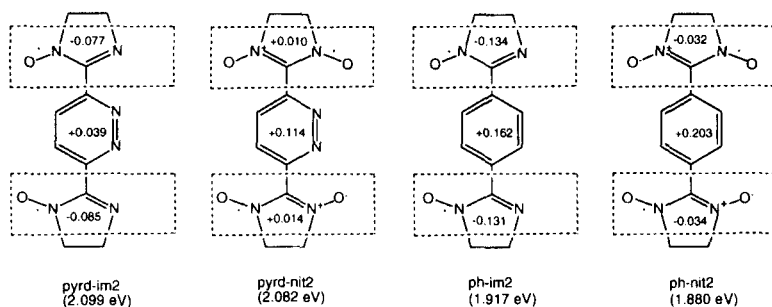


FIGURE 5. Net charge analyses for diradicals obtained by PM3 MO calculations. Numerical values in the parentheses are homo-lumo energy gaps.

### $K[Mn_2(\mu-CrO_4)_2(\mu-OH)_2]$ **3**.

Temperature dependent magnetic susceptibilities for **3** have been measured down to 2.0 K. Figure 6 shows both  $\chi_{Mn}$  and  $\chi_{Mn}T$  values vs.  $T$  plots. As the temperature is lowered, the  $\chi_{Mn}T$  values decrease and approach zero at 0 K, while the  $\chi_{Mn}$  values show a gradual increase with a slight undulation at 30 K. The magnetic behavior for **3** suggests that an antiferromagnetic interaction is operative. An analytical expression for the delocalized spin system of Mn(II,III) ions has not been developed, therefore, the system was treated as the alternate spin system of Mn(II) and Mn(III) ions. The data were analyzed recognizing that **3** has a one dimension like structure along the  $b$ -axis. First we analyzed the magnetic data by the Mn(II)-Mn(III) ferrimagnetic chain model derived by Drillon et al., where interchain interactions were included as a mean field correction.<sup>17</sup> The least squares calculation gave best fit parameters of intrachain ( $J_1$ ) and interchain ( $J_2$ ) coupling constants of  $-5.2(1)$  and  $-8.4(1)$   $cm^{-1}$ , with  $g$  values of  $2.0(1)$  and  $2.06(1)$  for Mn(II) and Mn(III) ions, respectively. Here  $H = -2J_1S_A \cdot S_B$  and  $\theta = 2zJ_2/3k$ .<sup>18</sup> The strength of the intrachain interaction is comparable to that of the interchain interaction, with  $|J_1/J_2| = 0.63$ . This does not satisfy the requirements of the mean field correction.

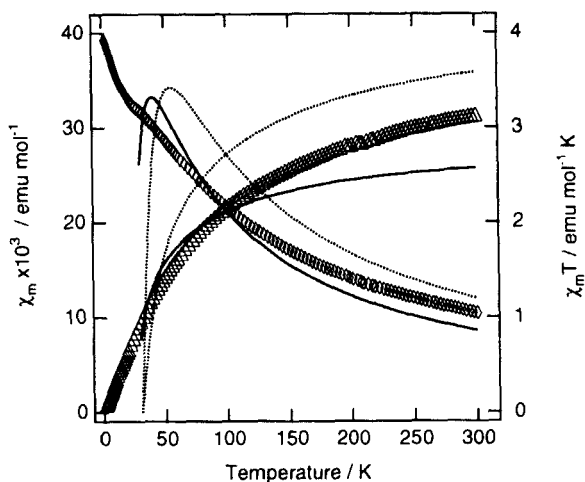


FIGURE 6. Plots of  $\chi_m T$  and  $\chi_m$  vs  $T$  for  $\text{K}[\text{Mn}_2(\mu\text{-CrO}_4)_2(\mu\text{-OH})_2]$  **3**. Solid lines correspond to the best fit curves by using the parameters given in the text.

High-temperature series expansions to a two-dimensional Heisenberg system was, therefore, applied to analyze the magnetic data.<sup>19</sup> When the 2D system has antiferromagnetic coupling, temperature dependent susceptibilities show a maximum value at  $T_{\text{max}}$ . The intra-layer coupling constant  $J$  can be estimated by the formula  $\tau_m = k_B T_{\text{max}} / JS(S+1)$  ( $\tau_m$  is a constant for different  $S$  values) and the molar susceptibility can be expressed as eq. 1,

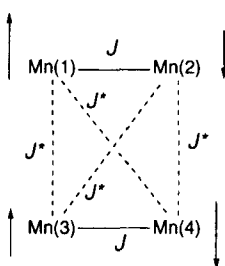
$$\chi_{\text{Mn}} = \frac{Ng^2\beta^2 S(S+1)}{3kT} \left( 1 + \sum_{n=1}^8 a_n K^n \right) \quad (1)$$

where  $K = J/kT$  and  $a_n$  values are taken from the previous work.<sup>20</sup> The  $\chi_{\text{Mn}}$  vs.  $T$  plot for **3** shows a fluctuation at 30 K. If the  $T_{\text{max}}$  value is taken as 30 K, then  $J$  is  $-1.4 \text{ cm}^{-1}$ . Figure 6 depicts theoretical curves for  $S = 2$  (solid line) and  $5/2$  (dotted line) systems with the  $g$  and  $J$  values of 1.97 and  $-1.4 \text{ cm}^{-1}$ , respectively. Clearly, experimental values above 100 K are between the range of the theoretical curves for the  $S = 2$  and  $S = 5/2$  spin systems. The least

square fitting of the data above 60 K with eq. (1) led to  $J = -1.8(1) \text{ cm}^{-1}$  and  $g$  1.97(1) with the  $S$  value being fixed to 2.25 ( $= (2+5/2)/2$ ).

In order to understand the magnetic structure of **3**, an rectangular core having a twofold axis with center of symmetry is cut out of the 2D layer structure. Two exchange parameters  $J$  and  $J^*$ , which represent coupling constants through O4 and O2-Cr-O2', and O2-Cr-O3' bridges, respectively, are required (Scheme).

Scheme



With  $J^*/J = 0$ , the Mn(1)-Mn(2) and Mn(3)-Mn(4) pairs are completely coupled. As  $J^*/J$  is increased, the Mn(1)-Mn(4) and Mn(2)-Mn(3) antiferromagnetic interactions frustrate the Mn(1)-Mn(3) and Mn(2)-Mn(4) antiferromagnetic interactions. The frustration prevents long range magnetic ordering and allows novel low temperature magnetic states to develop,<sup>21</sup> thus explaining the absence of the antiferromagnetic order in **3**.

## CONCLUSION

In summary, we have synthesized two new double-stranded radical helicates of silver imino nitroxides. Experimental results and PM3 MO calculations suggest that in diradical molecules an introduction of the more electronegative atoms into linking groups prompt spin delocalization, hence, the stronger magnetic interaction. It is also suggested by the MO calculation that spin on imino nitroxides is more delocalized onto the linking aromatics than nitronyl

nitroxides, and the stronger magnetic interaction through the bridges is expected for the imino nitroxides. This approach offers promising perspectives on synthesizing novel magnetic materials like helical and chiral magnets.

On the other hand, we have synthesized a 2D mixed valent Mn(II,III) complex with chromate bridges. It is expected that band filling of the system can be controlled by the introduction of different metal ions. More effort has been justified to prepare chromato-bridged hetero-metal complexes which might be a magnetic metal

## References

- [1] a) J.-M. Lahn, *Supramolecular Chemistry*, VCH, Weinheim, 1995. b) V. Balzani, *Tetrahedron*, **48**, 10443 (1992). c) E.C. Constable, *Tetrahedron*, 1992, **48**, 10013 (1992). d) A. Williams, *Chem. Eur. J.* **3**, 15, (1997).
- [2] a) P.N.W. Baxter, J.-M. Lehn, J. Fischer, M.-T. Youinou, *Angew. Chem. Int. Ed. Engl.* **33**, 2284 (1994).
- [3] a) J.-M. Lehn, A. Rigault, *Angew. Chem. Int. Ed. Engl.* **27**, 1095 (1988); b) R. Ziessel, A. Harriman, J. Suffert, M.-T. Youinou, A. De Cian, J. Fisher, *Angew. Chem. Int. Ed. Engl.* **36**, 2509 (1997). c) K.T. Potts, M. Keshavarz-K. F.S. Tham, K.A.G. Raiford, C. Arana, H.D. Abruna *Inorg. Chem.* **32**, 5477 (1993).
- [4] a) R.F. Carina, G. Bernardinelli, A.F. Williams, *Angew. Chem. Int. Ed. Engl.* **32**, 1463 (1993). b) C. Piguet, G. Bernardinelli, B. Bocquet, O. Schaad, A.F. Williams, *Inorg. Chem.* **33**, 41 12 (1994).
- [5] a) M.W. Wemple, H.-L. Tsai, S. Wang, J.P. Claude, W.E. Streib, J.C. Huffman, D. N. Hendrickson, G. Christou, *Inorg. Chem.* **35**, 6437 (1996). b) J.K. McCusker, H. G. Jang, S. Wang, G. Christou, D.N. Hendrickson, *Inorg. Chem.*, **31**, 1987 (1992). c) E. Libby, J.K. McCusker, E.A. Schmitt, K. Folting, D.N. Hendrickson, G. Christou, *Inorg. Chem.*, **30**, 3486 (1991).
- [6] E.M. Chudnovsky, *Science*, **274**, 938 (1996). b) R. Sessoli, D. Gatteschi, A. Caneschi, M.A. Novak, *Nature*, **365**, 141 (1993).
- [7] a) S.M.J. Aubin, M.W. Wemple, D.M. Adams, H.-L. Tsai, G. Christou, D.N. Hendrickson, *J. Am. Chem. Soc.*, **118**, 7746 (1996). (b) Stamp, P.C.E.; *Nature*, **383**, 125 (1996).
- [8] H. Oshio, T. Kikuchi, T. Ito, *Inorg. Chem.*, **35**, 4938 (1996).
- [9] H. Oshio, T. Kikuchi, T. Ito *norg.Chem.* **6**, 3201 (1997).
- [10] P. Chaudhuri, M. Winter, K. Wieghardt, S. Gehring, W. Haase, B. Nuber, J. Weiss, *Inorg. Chem.* **27**, 1564 (1988).
- [11] H.D. Flack, *Acta Crystallogr.* **A39**, 876 (1944).
- [12] The least squares calculation with the J1 and J2 values as variables for 2 gave unreasonable values of -86 and +45 cm<sup>-1</sup>, respectively. in spite of fact that the amplitudes of the J1 value should be close to -1.4 cm<sup>-1</sup>.
- [13] H.M. McConnell, *J. Chem. Phys.* **39**, 910 (1963).
- [14] A. Caneschi, P. Chiesi, L. David, F. Ferraro, D. Gatteschi, R. Sessoli, *Inorg. Chem.*, **32**, 1445 (1993).
- [15] PM3 MO calculations were done by MOPAC 6.0 for Machintosh. Structural parameters were optimized, where the dihedral angles of radical moiety and aromatic groups were fixed to 30°.
- [16] O. Kahn, "Molecular Magnetism", VCH publishers, (1993).
- [17] Drillon, M.; Corinado, E.; Beltran, D.; Gerge, *R Chem. Phys.*, **79**, 449 (1983).
- [18] Rose, N.R.; Stenkamp, R.; Willett, R.D. *Inorg. Chem.*, **30**, 4082 (1991).

- [19] "Magnetic Properties of Layered Transition Metal Compounds" Edited by de Jongh, L.J. Kluwer Academic Publishers, (1990).
- [20] a) Rushbrooke, C.S.; Wood, P.J. *Proc. Phys. Soc. London*, **68**, 1161 (1956). b) P. L. Stephenson, K. Pirnie, P.J. Wood, J. Eve *Phys. Lett.*, 27A, 2 (1968).
- [21] a) Fazekas, P.; P.W. Anderson, *Philos. Mag.*, **30**, 423 (1974). (b) Wannier, G.H. *Phys. Rev.*, **B7**, 5017 (1973).